Bidirectional Transformerless EV Charging System via Reconfiguration of 4x4 Drivetrain

Liwei Zhou, Matthias Preindl

Department of Electrical Engineering, Columbia University

New York City, NY, USA

Abstract− Electric vehicles (EV) are developing fast and EV ownerships are increasing rapidly. In the EV system, the electric traction inverter and the charging converter are two important components that will largely determine the performance of the EV. The research targets transformer-less integrated charging systems that have the potential to reduce the cost, volume, and increase efficiency. The proposed concept does not require a charging rectifier or isolating transformer and admits bidirectional operation that is the basis for providing V2G services to the grid. The omission of galvanic isolation permits common mode currents in the charging system during charging mode since both grid and vehicle chassis are grounded during charging. These currents are well controlled using a secondary converter that acts as an active filter. Furthermore, the omission of the isolating transformer increases the efficiency of the vehicle charger similar. The proposed topology is verified by simulation and on an experimental test bench.

I. INTRODUCTION

The electric vehicle is entering a fast developing period. The design of the charging and traction systems for the EV is of great importance. [1] Because the charger and traction inverter do not work in the same period of time, for the purpose of saving the volume and weight of the whole system, the charger and traction are expected to share the same converter to perform a bi-directional power flow. [2] The integrated charging system for the EV can use the traction inverter to charge the battery from the grid with the bi-directional power delivering ability. And as the development of EV market, the grid also requires the EV to provide V2G service for the mitigation of grid power fluctuation. [3] However, because the grid is grounded, during the charging and V2G mode, there exists the common mode noise between the ground and the EV circuits which may threaten the safety of the system. Some standards have made the limitations for the common mode noise or dc current injection into the grid. [4-6] A transformer can be applied to isolate the common mode noise. Some papers also contribute to design this type of isolated topology for the attenuation of common mode noise. However, it will largely increase the volume and weight due to the transformer. On the other hand, some kinds of transformer-less topologies have also been proposed to reduce the common mode noise in a single inversion circuit. The disadvantage of this idea is that it will cost extra devices to bypass the freewheeling current.

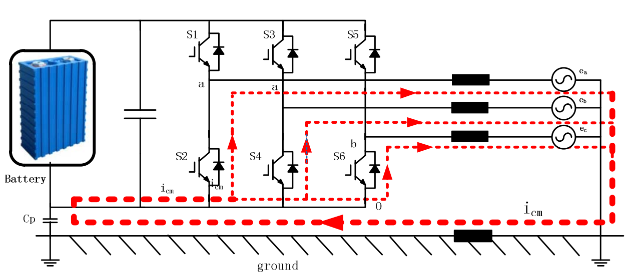

Fig. 1. The common-mode circuit of the EV during charging or V2G modes

In this paper, a novel multiplex integrated charging system is proposed to attenuate the common mode noise without increasing the whole volume and cost. The proposed system applies the typical paralleled traction topology of four-wheel-drive EV circuit to largely reduce the common mode noise during charging and V2G mode. No extra switches are needed which will save the device cost. Firstly, the equivalent common mode circuit in the EV is analyzed. Secondly, the proposed novel integrated charging topology is introduced with the analysis of the operational principle. Then, another different topology for single phase charging mode is analyzed. Finally a comparison between the novel topologies and the traditional topologies is illustrated to verify the advantages of the proposed system.

II. ANALYSIS OF COMMON-MODE NOISE IN INTEGRATED ELECTRIC VEHICLE SYSTEM

In this section, the common mode noise of the integrated electric vehicle system is analyzed. [7] Fig. 1 shows the common mode leakage current paths during the charging or V2G modes. For the consideration of cost and volume, this paper focuses on the transformer-less inversion system. So the lack of isolation transformer results in a path of common-mode leakage current consisting of the parasitic capacitance between the ground, battery and the EV circuit. The six switches of the inverter work in high frequency, which causes a common-mode voltage u_{cm} during the operation period. [8] Fig. 2 shows the equivalent circuit of three phase inverter. The bridge arm voltages are replaced with the differential voltages, u_a, u_b and u_c. The common mode voltage is replaced with a high frequency voltage pulse, u_{CM}. The fluctuation of u_{cm} will generate a common-mode leakage current in the paths of common-mode circuit. [9] The

TABLE I
COMMON MODE BEHAVIOR OF TRADITIONAL 3-PHASE INVERTER

Mode		u_{an}	u_{bn}	u_{cn}	u_{cm}
Active states	100	u_{dc}	0	0	$u_{dc}/3$
	010	0	u_{dc}	0	$u_{dc}/3$
	001	0	0	u_{dc}	$u_{dc}/3$
	110	u_{dc}	u_{dc}	0	$2u_{dc}/3$
	011	0	u_{dc}	u_{dc}	$2u_{dc}/3$
	101	u_{dc}	0	u_{dc}	$2u_{dc}/3$
Null states	111	u_{dc}	u_{dc}	u_{dc}	u_{dc}
	000	0	0	0	0

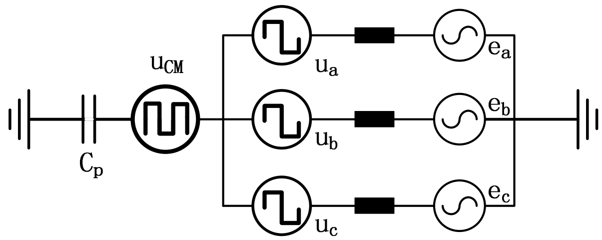

Fig. 2. The equivalent circuit of three phase inverter

definition of u_{cm} can be calculated as:

$$u_{CM} = \frac{u_{an}+u_{bn}+u_{cn}}{3} \quad (1)$$

In equation (1), u_{an}, u_{bn} and u_{cn} are the pulsating voltage between the output of the bridge and the negative trail of DC side, respectively. The value of common-mode leakage current i_{cm} is induced by the fluctuation of u_{cm}. The leakage current can be expressed with the derivative of common mode voltage:

$$i_{cm} = C_{PV}\frac{du_{cm}}{dt} \quad (2)$$

The calculation of common mode voltage in equation (1) shows that each combination of switching state for the three phase inverter is corresponding to a specific value of common mode voltage. The common mode voltages of all switching states are given in Table I, where the common mode voltage varies among four levels: 0, $u_{dc}/3$, $2u_{dc}/3$, u_{dc}. Three phase inverter has 8 switching states. For example, if the switches S1, S3 and S6 are ON, the switching state can be expressed as (110). In this working mode, the common mode voltage can be calculated as: $(u_{dc}+u_{dc}+0)/3=2u_{dc}/3$. It can be observed from Table I that the maximum and minimum value of the CM voltages are u_{dc} and 0 which are corresponding to the two null states (111) and (000), respectively.

To conclude for the suppression of leakage current in the three phase inverter, one effective way is to reduce the fluctuation range of the CM voltage. Although several methods have been proposed to eliminate the common mode voltage, most of the ideas are based on the modulation strategies of the traditional three-level NPC inverter. However, the NPC inverter has twelve switches and six diodes which costs lots more devices than the traditional two level inverter in Fig. 1. Also, the conducting losses of the NPC inverter is higher than the two level inverter. In the following sections of this paper, the proposed reconfiguration topologies can reduce the leakage current without using extra devices and the conduction losses are lower than the traditional NPC inverter.

III. MULTIPLEX APPLICATION OF CHARGING SYSTEM IN REDUCTION OF COMMON MODE NOISE

The proposed integrated charging system with low common mode noise is introduced in this section. Firstly, the typical structures of integrated charging system for electric vehicle are introduced including the rear-wheel drive and four-wheel drive EV systems. Then two kinds of novel integrated charging/V2G EV topologies with low common mode noise are proposed. The working principles are also analyzed.

A. The typical structure of integrated charging system for electric vehicle

Fig. 3 shows the typical structure of integrated plug-in on-board EV system with rear-wheel drive. The system includes the battery, DC/DC converter, bi-directional converter and motor. [10-11] During the traction mode, the bi-directional converter works as an inverter to drive the motor of the rear wheel. In the charging mode, the bi-directional converter works as a rectifier to deliver the power from the grid to the battery. Also, if V2G service is provided by the EV, the power can also flow from the battery to the grid. The power flow paths are labeled by the arrows in the figure. According to the direction of the power flow, the working modes of the system can be divided into charging mode and V2G/traction mode as is shown in Fig. 2. [12]

Furthermore in this paper, we focus on the 4x4 drivetrain system. Fig. 4 shows the typical structure of integrated charging system of four-wheel drive EV. [13] Different from Fig. 3, two traction converters are connected to the battery in parallel. The power can also flow from grid to battery through one of the three phase converter as is analyzed in Fig. 3. So for the four-wheel drive traction system in Fig. 4, one converter is bi-directional to deliver power from battery to grid in traction/V2G modes and from grid to battery in charging mode. The other converter is only operating in traction mode to drive the front wheels.

B. The proposed integrated charging system for three phase charging mode application

The proposed topology is shown in Fig. 5 which includes two main components: two sets of paralleled three phase converters. The left sides of the two converters are connected in parallel and both are connected to the battery through a DC/DC converter. The right sides of the two converters are connected to the front-wheel motor and rear-wheel motor respectively. Also, in the proposed system, the outputs of the two converters' phase legs are connected by three relays which will be closed during the charging or V2G mode to

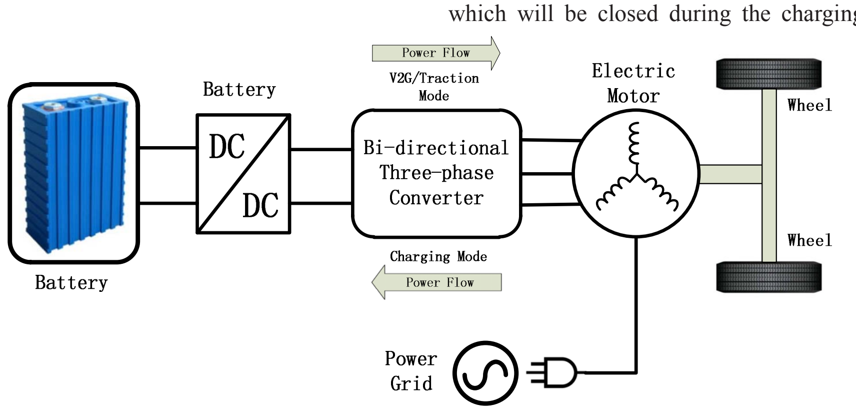

Fig. 3. Typical structure of integrated plug-in on-board EV system with rear-wheel drive.

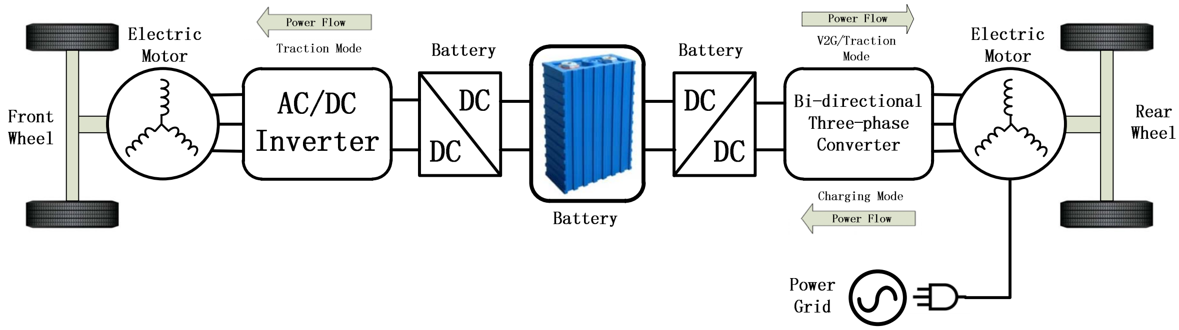

Fig. 4. Typical structure of integrated plug-in on-board EV system with four-wheel drive.

attenuate the common mode noise. Following are the working principles of the proposed charging topology in different operation modes.

Firstly, in the traction mode, the relays, R_{1-3}, are disconnected. The two converters are working individually to drive the two motors as is shown in Fig. 5. Secondly, in the charging mode or the V2G mode as is shown in Fig. 6, the relays, R_{1-3}, are closed and the battery is transferring energy with the grid through the rear-wheel motor converter during the energy transferring period. In addition, the DC side relay of the front-wheel converter is disconnected to avoid the influence of the DC voltage. And in the freewheeling period, the six switches of the rear-wheel converter are OFF. The three upper switches (S1', S3', S5') of front-wheel converter are connected to the grid by the three lines and relays to provide the freewheeling paths for the converter. Thus, the output of the converter has a three level voltage and the common mode voltage can be largely reduced. The analysis for the attenuation of common mode noise is illustrated below.

Considering the attenuation of the common mode voltage, the null states of the traditional two level three phase inverter are improved and modified with the additional freewheeling circuit provided by three upper switches (S1', S3', S5') of front-wheel converter. In the traditional SPWM, the two null states are (111) and (000), which can be realized by turning on the three upper switches, S1, S3 and S5 or the three lower switches, S2, S4 and S6. However, in these two situations, the common mode voltages have the maximum and minimum values which will increase the fluctuating ranges of the common mode voltage, thus the leakage current can be

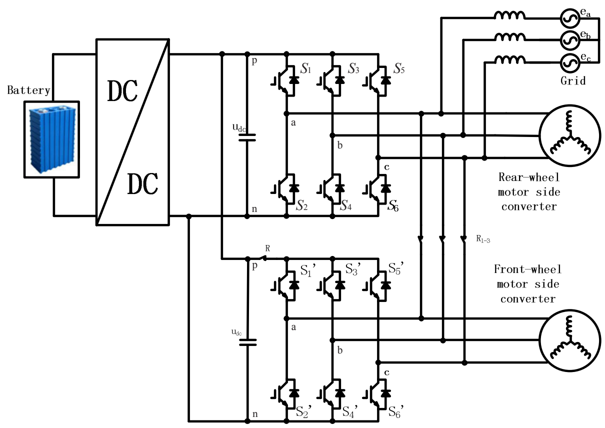

Fig. 5. Proposed integrated three phase charging topology for four-wheel drive.

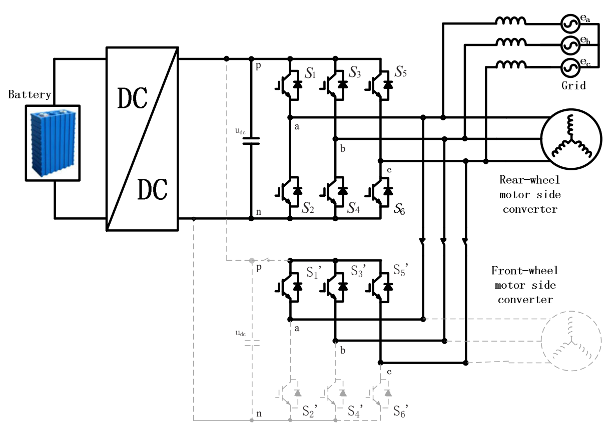

Fig. 6. Charging or V2G modes of proposed integrated three phase charging topology for four-wheel drive.

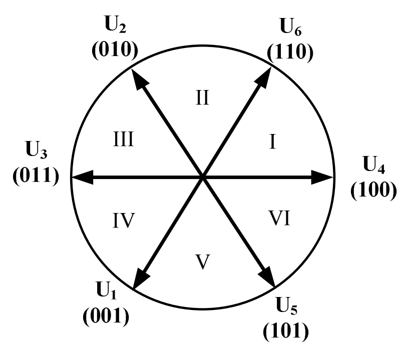

(a)

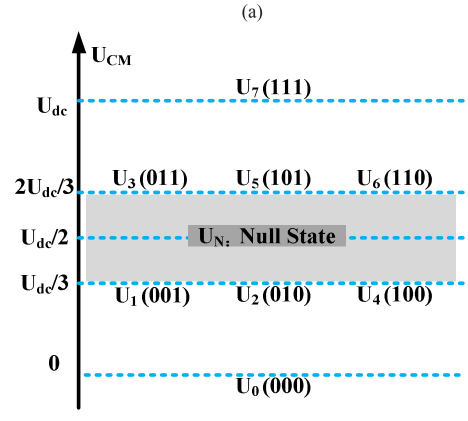

(b)

Fig. 7. (a) The vectors of the traditional six active switching states; (b) the comparison of the common mode voltage ranges between the traditional three phase inverter and the proposed charging topology.

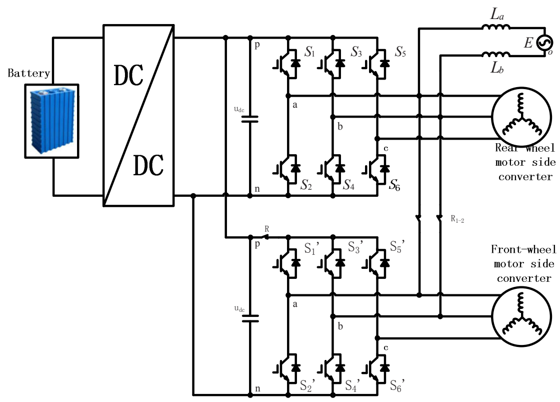

Fig. 8. Proposed integrated single phase charging topology for four-wheel drive.

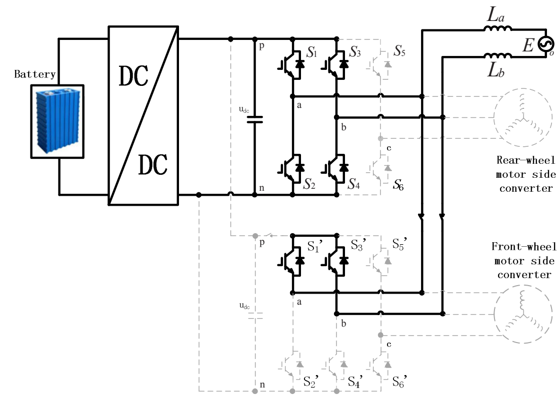

Fig. 9. Charging or V2G modes of proposed integrated single phase charging topology for four-wheel drive.

increasing significantly. In the novel topology shown in Fig. 6, the null states of (111) and (000) are replaced by turning on the three upper switches (S1', S3', S5') of front-wheel converter. Doing so, the common mode voltages of the null states, 0 and u_{dc}, are eliminated and replaced by the new freewheeling circuit. During the freewheeling period of the charging/V2G modes, the three switches, S1', S3' and S5', are ON and the switches of the three bridge legs, S_1-S_6, are OFF. In this situation, the potentials between the output points of three phase legs, a, b, c and the negative point of the DC link are all $u_{dc}/2$. Thus the common mode voltage is $(u_{dc}/2+ u_{dc}/2+ u_{dc}/2)/3= u_{dc}/2$.

The comparison of the common mode voltage ranges between the traditional three phase inverter and the proposed charging topology is shown in Fig. 7. Fig. 7(a) expresses the six vectors of the active switching states. Furthermore, it can be easily derived from Fig. 7(b) that the peak to peak value of the common mode voltage can be reduced from u_{dc} to $u_{dc}/3$ as is shown in the central grey region. Thus the leakage current will be significantly attenuated.

C. The proposed integrated charging system for single phase charging system

Also, for the single phase charging mode or the V2G service for single phase grid, a novel charging system using the anti-series connected switches of the front-wheel motor converter is shown in Fig. 8 to eliminate the common mode noise without extra device cost.

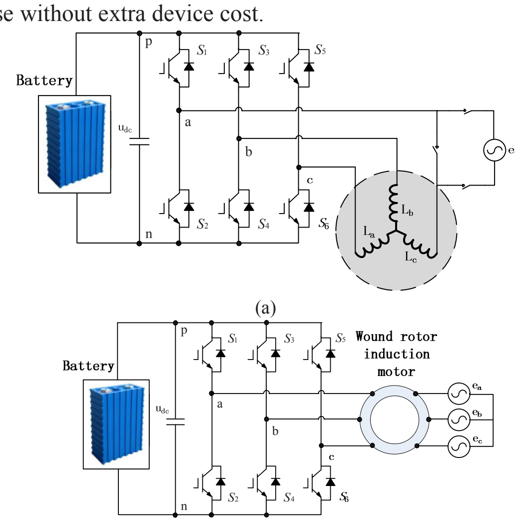

(a)

(b)

Fig. 10. Integrated charger system based on (a) induction motor (b) wound rotor.

In Fig. 8, the outputs of the phase A and phase B of the two three-phase converters are connected by two lines and delays. Firstly, in the traction mode, the relays, R_{1-2}, are OFF. The two converters are working individually to drive the front and rear motors. Secondly, in the charging or the V2G modes as is shown in Fig. 9, the rear-wheel converter will be connected to the single phase grid with the bridge A and bridge B. In this case, only S1-S4 of rear-wheel converter are working. Also, the anti-series connected upper switches (S1', S3') of the front-wheel converter will deliver the freewheeling current due to the connection of relays, R_{1-2}. The DC side relay is disconnected in this period to avoid the influence of the DC voltage. Thus, the common mode voltage of the proposed single phase charging system in Fig. 9 is $(u_{dc}+ 0)/2= u_{dc}/2$ in the energy transferring mode and $(u_{dc}/2+ u_{dc}/2)/2= u_{dc}/2$ in the freewheeling mode. Thus, the common mode voltage is remained constant during the whole charging/V2G period. According to equation (2), the common mode noise can be largely attenuated.

D. Comparison with other topologies

This section compares the proposed integrated charging systems with other EV charging topologies. Fig. 10 and Fig. 11 show the typical integrated charging system which have already existed. It can be seen from Fig. 10(a) that the charging topology has no isolation thus the common mode current will be in a high level. Similarly in Fig. 11, the split windings can not solve the common mode noise either. And

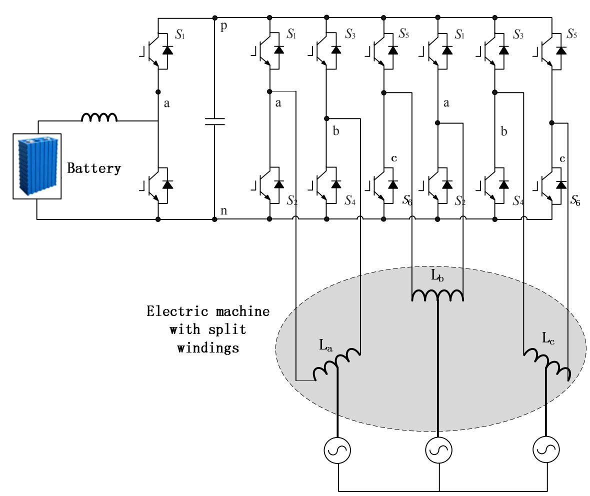

Fig. 11. Integrated charger system based on split-windings.

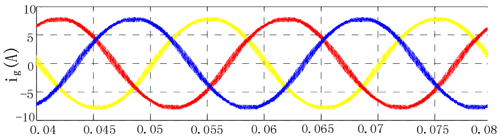

Fig. 12. The output current of the proposed three phase inverter.

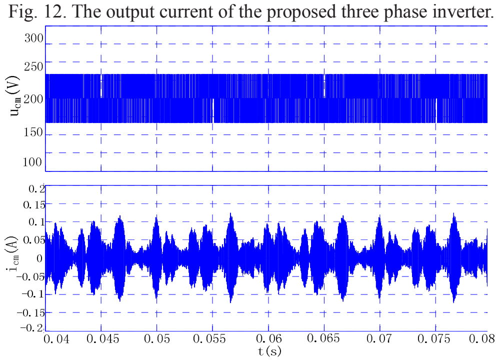

Fig. 13. The common mode voltage and leakage current of the proposed three phase charging system in Fig. 6.

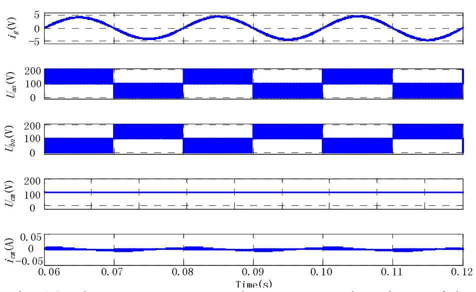

Fig. 14. The output current and common mode voltage of the proposed single phase charging system in Fig. 9.

the device cost is twice as the traditional three phase converter. In Fig. 10(b), the wound rotor induction motor uses the transformer to isolate the leakage current which will increase the system volume and weight.

On the other hand, the proposed topologies will not increase any extra switches to eliminate the common mode voltage. Also the conduction loss of the novel circuit is low compared to other three level NPC inverters which will increase the efficiency of the conversion system.

IV. SIMULATION AND EXPERIMENTAL RESULTS

The simulation and experimental results are shown in this section to test the output current and common mode noise of the proposed charging topologies. The proposed integrated charging system was simulated in Matlab/Simulink and experimentally validated on a 2kW test bench.. The DC voltage is 400V (three phase) and 200V (single phase) and the grid voltage is 110V/50Hz. The switching frequency for the inverter is 10 kHz. The output inductors are 2mH. The grid current is controlled by a conventional PR controller. Fig. 12-13 are the grid current and common mode characteristics of the proposed three phase system in Fig. 6. Fig. 14-15 are the common mode characteristics for the proposed single phase charging system in Fig. 9. From the common mode results of Fig. 13, 14 and 15, the common mode voltage u_{cm} is reduced to 1/3 of the DC voltage in three phase inverter and remained constant as 1/2 of the DC voltage in single phase inverter respectively. Thus the common mode noise is largely attenuated.

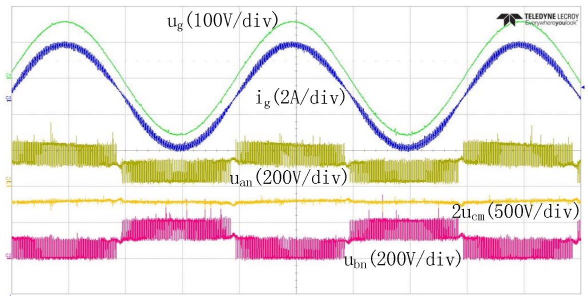

Fig. 15. The experimental waveforms of proposed single phase common mode voltage, phase leg voltages leakage current and output current .

V. CONCLUSION

This paper proposed a multiplex application for integrated charging topology in EV system. The novel topologies use the intrinsic switches to create extra freewheeling paths for the attenuation of common mode noise. The weight and volume of the system are largely saved without the isolating transformer. The conduction loss and device cost are low. The simulation and experimental results verified The simulation and experimental results verified that the common mode voltages in the proposed single phase and three phase topologies are constant which results in a low level of common mode noise.

VI. ACKNOWLEDGEMENT

This research is based in part upon work supported by National Science Foundation under Grant Number 1653574.

REFERENCES

[1] M.Yilmaz and P. T.Krein, "Review of battery charger topologies, charging power levels, and infrastructure for plug-in electric and hybrid vehicles," *IEEE Trans. Power Electron.*, vol. 28, no. 5, pp. 2151–2169, May 2013.

[2] Y. Du, S. Lukic, B. Jacobson, and A. Huang, "Review of high power isolated bi-directional DC-DC converters for PHEV/EV DC charging infrastructure," in *Proc. IEEE Energy Conversion Congr. Expo.*, Sep. 2011, pp. 553–560.

[3] X. Zhou, G. Wang, S. Lukic, S. Bhattacharya, and A. Huang, "Multifunction bi-directional battery charger for plug-in hybrid electric vehicle application," in *Proc. IEEE Energy Conversion Congr. Expo.*, Sep. 2009, pp. 3930–3936.

[4] VDE 0126-1-12006: "Automatic disconnection device between a generator and the public low-voltage grid, " DIN_VDE Normo, 2008.

[5] *Power Quality Requirements for Plug-in Vehicle Chargers—Part 1: Requirements*, SAE International Standard J2894, 2011.

[6] *Electromagnetic Compatibility (EMC)—Part 3: Limits—Section 2: Limits for Harmonic Current Emissions*, IEC1000-3-2 Doc., 1995.

[7] L. Zhou, F. Gao, and T. Xu, "Implementation of Active NPC Circuits in Transformer-Less Single-Phase Inverter With Low Leakage Current", *IEEE Trans. Ind. Appl.*, vol. 53, no. 6, pp. 5658-5667, 2017.

[8] L. Zhou, F. Gao, and T. Xu, "A family of neutral-point-clamped circuits of single-phase PV inverters: Generalized principle and implementation," IEEE Trans. Power Electron., vol. 32, no. 6, pp. 4307–4319, Jun. 2017.

[9] Ivan Echeverria, Fernando Arteche, Mateo Iglesias, Alvaro Pradas, Javier Piedrafita and Francisco Javier Arcega, "Common Mode Noise Propagation and Effects in a Four-Wheel Drive Electric Vehicle," IEEE Trans. Electromagn. Compat., vol. 60, no. 1, pp. 132–139, Feb. 2018.

[10] L. Zhou, F. Gao, "Improved transformerless dual buck inverters with buffer inductors," in *Proc. IEEE Applied Power Electronics Conference and Exposition (APEC)*, Mar. 2016, pp. 2935–2941.

[11] S.-K. Sul and S.-J. Lee, "An integral battery charger for four-wheel drive electric vehicle," *IEEE Trans. Ind. Appl.*, vol. 31, no. 5, pp. 1096–1099, Sep./Oct. 1995.